

## MONTE CARLO SIMULATION OF A HEMT STRUCTURE

Claudiu AMZA, Ovidiu-George PROFIRESCU, Ioan CIMPIAN, Marcel D. PROFIRESCU

EDIL Microelectronics and Nanoelectronics R&D Centre of Excellence, University Politehnica of Bucharest, Romania  
E-mail: claudiu@edil.pub.ro, ovidiu@edil.pub.ro, black@edil.pub.ro, profires@edil.pub.ro

The paper presents an analysis of a pseudomorphic HEMT structure through an ensemble Monte Carlo simulation. The effect of velocity overshoot and real-space transfer on the device performance is investigated. The electron drift velocity drops due to the intervalley transfer in the bulk InGaAs, and real-space transfer into the surrounding lower mobility GaAs and AlGaAs layers. Depending on the gate bias, the velocity near the drain is limited by either k-space or real-space transfer. At low gate bias real-space transfer occurs, while at high gate bias intervalley transfer within the bulk InGaAs limits the carrier speeds.

### 1. INTRODUCTION

Over the last three decades the Monte Carlo (MC) method has evolved to a reliable and frequently used tool which has been successfully employed to investigate a great variety of transport phenomena in semiconductors.

The method consists of a simulation of the motion of charge carriers in the six-dimensional phase space formed by the position and wave vectors. Subjected to the action of an external force, the point-like carriers follow trajectories determined by Newton's law and the carrier's dispersion relation. Due to imperfections of the crystal lattice the drift process is interrupted by scattering events, which are considered to be local in space and instantaneous in time. The duration of a drift process and the type of scattering mechanism are selected randomly according to given probabilities which describe the microscopic process. In principle, such a procedure yields the carrier distribution in phase space. Integrating the distribution function over some phase space volume gives a measure for the relative number of carriers in that volume. Macroscopic quantities are obtained as mean values of the corresponding single-particle quantities. Moreover, the distribution function satisfies a Boltzmann equation (BE). The method of generating sequences of drift and scattering appears so transparent from a physical point of view that it is frequently interpreted as a direct emulation of the physical process rather than as a numerical method. The main MC algorithms used to date were originally devised from merely physical considerations, viewing a MC simulation as a simulated experiment. The proof that the used algorithms implicitly solve the BE was carried out later. The alternative way to use the BE explicitly and to formulate MC algorithms for its solution was reported only one decade ago in the literature. New MC algorithms are derived which typically differ from the common ones by the fact that additional statistical variables appear, such as weights, that do not have a counterpart in the real statistical process.

### 2. MONTE CARLO METHOD FOR SEMICONDUCTOR DEVICES

Based upon the physical picture of the MC technique it has been possible to apply the method to the simulation of a great variety of semiconductor devices. When the need for variance reduction techniques

emerged these have again been devised from physical considerations, like splitting a particle into light ones by conserving the charge.

Transient phenomena are due to the evolution of the carrier system from an initial to some final distribution. Accordingly, the evolution of an ensemble of test particles is simulated starting from a given initial condition. The physical characteristics are obtained in terms of ensemble averages, giving rise to the name Ensemble MC [1]. For example, the distribution function in a given phase space point at a given time is estimated as the relative number of particles in a small volume around the point.

The EMC algorithm can also be applied under stationary conditions. In this situation, for large evolution times the final distribution approaches a steady-state, and the information introduced by the initial condition is lost entirely. Alternatively, the ergodicity of the process can be exploited to replace the ensemble average by a time average. Since it is sufficient to simulate one test particle for a long period of time, the algorithm is called one-particle MC. The distribution function in a given phase space point is estimated by the time spent by the particle in a fixed, small volume around the point divided by the total time the trajectory was followed. The effect of the particle's initial state vanishes for long simulation times. Another method of obtaining steady-state averages has been introduced by Price [2]. With the synchronous-ensemble or before-scattering method averages are formed by sampling the trajectory at the end of each free flight, which is in many cases easier a task than evaluating a path integral over each free flight. When the EMC algorithm is applied to the simulation of a stationary phenomenon, the steady-state is reached after the initial transient has decayed. The ensemble average is taken at the end of the simulation time, while, on the contrary, with the OPMC algorithm averages are recorded during the whole time of simulation.

For the inhomogeneous situation the mathematical model needs to be augmented by boundary conditions. Physical models for Ohmic contacts typically enforce local charge neutrality. The EMC and the OPMC algorithms remain basically unchanged in the inhomogeneous case. Whenever in an OPMC simulation a particle leaves the simulation domain through an Ohmic contact it is re-injected through one of the contacts, selected according to the probabilities of the underlying model.

The work of Kurosawa in 1966 is considered as the first account of an application of the MC method to high-field transport in semiconductors. The following decade has seen considerable improvement of the method and application to a variety of materials. The used band structure models were represented by simple analytic expressions accounting for non-parabolic bands and anisotropy. With the increase of the energy range of interest the appears the need for accurate, numerical band structure models. Using Monte Carlo method we can study various technologically significant semiconductors and alloys.

The high electron mobility transistor (HEMT) structures are highly used in high-power millimeter-wave applications. The HEMT's superior performance comparing with conventional MESFET structures has been demonstrated in both analog and digital integrated circuits. The advantages of the HEMT comes from the use of modulation doping. In this way, significant current is delivered by the device without scarifying speed by spatially separating the donor atoms from the current-carrying channel. As in a MOSFET, the channel in a HEMT is formed at the interface between two semiconductor materials of different energy band-gaps. Electrons transfer from the highly doped wide band-gap layer into the intrinsic low-gap layer where they are confined in a potential well due to the band bending at the interface. The electrons thus form a two-dimensional electron gas within the channel in which the electron mobility exceeds that of comparable bulk material. The spatial separation of the current-carrying charge from the donor impurity atoms and the intrinsic high mobility of a two-dimensional system provide excellent high-speed performance. [3]

The performance of AlGaAs/GaAs HEMTs is lowered by the photoconductivity effect, threshold voltage change with temperature, drain  $I$ - $V$  characteristic collapse, and generation-recombination noise, which appear within high Al content heterostructures due to shallow and deep donors in AlGaAs.

These limitations of conventional AlGaAs/GaAs HEMTs leads to the development of strained layer pseudomorphic  $\text{In}_{0.15}\text{Ga}_{0.85}\text{As}/\text{GaAs}$  and  $\text{Al}_{0.15}\text{Ga}_{0.85}\text{As}/\text{In}_{0.15}\text{Ga}_{0.85}\text{As}$  devices.

The pseudomorphic HEMTs have a large conduction band edge discontinuity between the AlGaAs layer and InGaAs channel with a lower aluminum mole fraction. In this way the persistent photoconductivity effect, threshold voltage change, and  $I$ - $V$  collapse can be avoided. Generation-recombination noise is reduced due to the reduction of occupied deep levels in low Al mole fraction AlGaAs. In AlGaAs/InGaAs/GaAs pseudomorphic HEMTs, the InGaAs channel leads to better device performance due to improved electron confinement within the two-dimensional quantum-well system.

### 3. DESCRIPTION OF THE SIMULATION FRAMEWORK

The transport physics of the two-dimensional electron gas from the heterostructure interface, the effects of real-space transfer and nonstationary transport, as well as that of the two-dimensional electrostatic potential are of great importance for the device analysis. The pseudomorphic AlGaAs/InGaAs/GaAs HEMT structure illustrated in Figure 1 has been used in the simulation. [2] In this device, it is assumed that the doping concentration of the unintentionally doped GaAs and InGaAs layers is  $3 \cdot 10^{15} \text{ cm}^{-3}$ . The electron concentration in the bulk is scaled to that of the  $\text{Al}_{0.15}\text{Ga}_{0.85}\text{As}$  system, which is  $3.0 \cdot 10^{18} \text{ cm}^{-3}$ . The two-dimensional electron gas concentration is  $1.1 \cdot 10^{12} \text{ cm}^{-2}$ . The electron concentration in the bulk is  $3.0 \cdot 10^{18} \text{ cm}^{-3}$ . The two-dimensional electron gas concentration is  $1.1 \cdot 10^{12} \text{ cm}^{-2}$ . The top-most layer consists of a 360-Å-thick  $3.0 \cdot 10^{18} \text{ cm}^{-3}$  doped,  $\text{Al}_{0.15}\text{Ga}_{0.85}\text{As}$  layer, followed by a 40 Å thick AlGaAs undoped spacer layer. The channel layer is between the AlGaAs layer to the top and an undoped GaAs layer below (180 Å undoped  $\text{In}_{0.15}\text{Ga}_{0.85}\text{As}$ ).

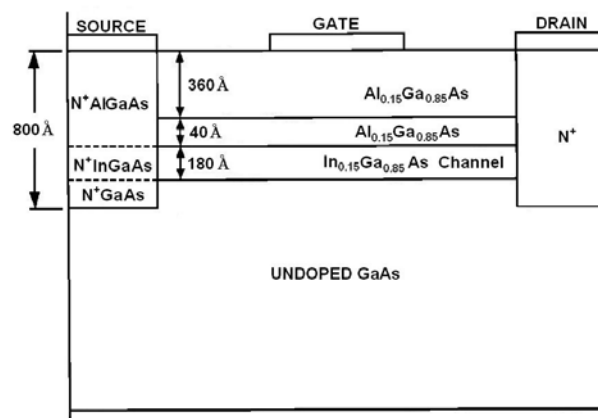


Fig.1. The pseudomorphic HEMT used in the simulation.

The simulations are performed using a many particle ensemble Monte Carlo coupled with a two-dimensional Poisson solver. The electron trajectories are followed in two dimensions in real space according to the relevant phonon and impurity scattering mechanisms present, as well as the action of the two-dimensional electric field profile. [3]

The local fields within each cell do not change instantaneously with the motion of the carriers. The field is adjusted after a finite time interval. Each carrier accelerates under the action of the two-dimensional electric field until a scattering event occurs or until the end of the field-adjusting time step is reached. The carriers move from one cell into another, changing the self-consistent field. The carriers will transit through no more than one cell interface on average before the field is updated. In this way the field is updated only where the rapidly changes exists.[6]

The boundary condition at the gate is specified by equation (1):

$$V_g = V_{ga} - r \frac{E_g}{q} + \frac{\Delta E_c}{q} - \frac{E_f}{q} \quad (1)$$

where  $V_{ga}$  is the applied gate voltage,  $\Delta E_c$  is the AlGaAs/InGaAs conduction band edge discontinuity,  $E_g$  is the energy bandgap of the AlGaAs layer,  $r$  is a parameter ranging from zero to one that specifies the point within the energy gap at which the surface or interface states lie, and  $E_f$  the Fermi energy. At the heterojunction interfaces between either the AlGaAs and InGaAs or the InGaAs and GaAs layers, the normal component of the electric field is discontinuous by the interface charge density  $n_s$ , and expressed by relations (2) and (3).

$$(\text{AlGaAs}) \left. \frac{d\phi}{dy} \right|_{y^+} + qn_s = \left. \frac{d\phi}{dy} \right|_{y^-} (\text{InGaAs}) \quad (2)$$

$$(\text{InGaAs}) \left. \frac{d\phi}{dy} \right|_{y^+} + qn_s = \left. \frac{d\phi}{dy} \right|_{y^-} (\text{GaAs}) \quad (3)$$

At the beginning of the simulation, the electron is launched in the source contact and moves within bulk InGaAs. After injection into the active region of the device, most of the electrons enter the channel. If the initial kinetic energy of the injected electrons exceeds the band-bending energy, the electrons enter either the two-dimensional electron gas system or the bulk InGaAs system [7].

The two-dimensional system is formed by the spatial confinement of the electrons due to the AlGaAs/InGaAs conduction band edge discontinuity on one side and the conduction band bending in the InGaAs layer on the other forming a triangular quantum well as shown in Figure 2.

Relation (4) gives the energy in the triangular well:

$$E = E_j + \frac{\hbar^2}{2m^* (k_x^2 + k_z^2)} \quad (3)$$

where  $E_j$  is the subband energy. The electron  $k$  vector component in the  $y$  direction remains fixed during its flight while the  $x$  and  $z$  components change according with the action of the applied electric field.

At electron energies greater than that corresponding to the band bending, the electrons are assumed to move within bulk InGaAs system. The electrons transfers to the two-dimensional states after drifting to lower energies, those below the band bending energy that defines the well height. The coupling of the two-dimensional system to the bulk is through polar optical phonon scatterings. At electron energies near the top of the quantum well, the electrons scatter within the bulk InGaAs. In the same way the electron enter the quantum-well system from the bulk via polar optical phonon emission events. The electron transfer from the quantum system to the bulk depends on the relative strength of the polar optical scattering within the two systems. Within the two-dimensional system, the electron motion is subject to various two-dimensional scattering mechanisms, particularly, polar optical. phonon, acoustic phonon, alloy, and remote impurity scattering [8]. In our simulation of the two-dimensional system, the subbands are assumed to form only in the gamma valley, and the  $L$  and  $X$  valleys are treated as three-dimensional since the intervalley separation energies for the  $L$  and  $X$  minima exceed the potential well height.

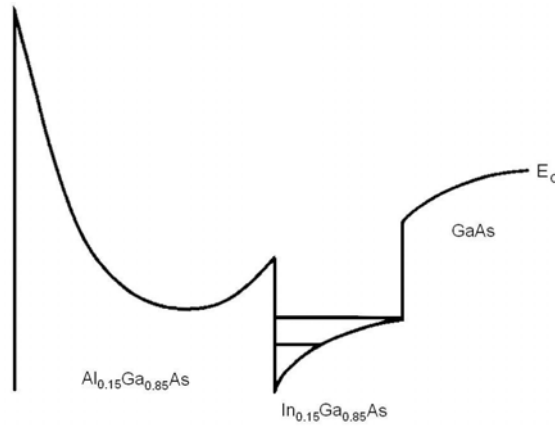


Fig. 2. The conduction band structure of the Al-GaAs/InGaAs/GaAs pseudomorphic HEMT

The overall two-dimensional scattering rates are calculated including both intra and inter-band scatterings.

The final state of the electron after suffering a two-dimensional scattering event is found in a similar way to that for bulk material except that the  $k$  vector component in the  $y$  direction remains fixed. However, the  $k$  vector component in the  $x$  and  $z$  directions changes in accordance with the scattering event. Therefore, only one scattering angle is necessary to determine the final state after a two-dimensional scattering. At low

electric field strengths, the carriers remain within the two-dimensional quantum well [5]. As the electric field increases, the electrons begin to transfer out of the two-dimensional system into the bulk InGaAs channel region. The electrons can be further heated to sufficiently high energy when real-space transfer into the surrounding AlGaAs or GaAs layers can occur. Under certain bias conditions, a significant portion of the drain current flows through a stray path in the AlGaAs layer. Due to the large concentration of impurities present and subsequently high scattering rate, the higher electron effective mass, and the loss of considerable kinetic energy upon crossing the heterojunction interface, the device performance is degraded when sizeable current flows within the AlGaAs layer. [9]

#### 4. RESULTS

The longitudinal electric field profile within the channel is plotted as a function of distance along the device for two different gate biases, 0.25 and 0.85 V, in Figure 3.

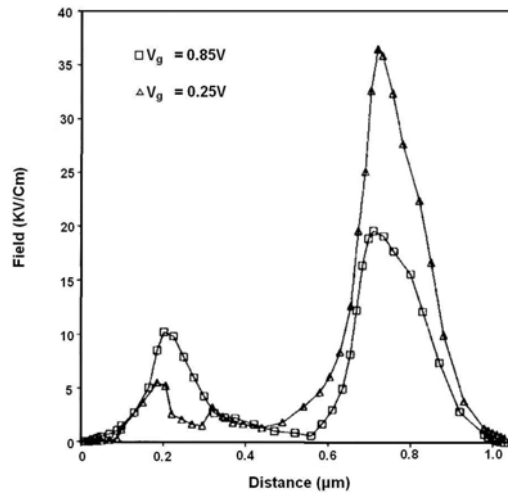


Fig. 3. Longitudinal electric field plotted as a function of distance along the device

The electric field is greater near the source at higher gate bias due to the fact that there is a greater potential difference established between the source and the gate under this condition. Due to the rapidly changing electric field throughout the device effects, such as velocity overshoot and ballistic transport can be observed.

The average carrier energy as a function of distance along the device is plotted for two different gate biases in Figure 4. A number of the electrons are heated to energies above that corresponding to the two-dimensional quantum well at the hetero-interface. This fact is explained by the abrupt increase of the electric field at the source-channel interface under high gate bias.

These carriers enter the bulk InGaAs system. Therefore, even under high gate bias, some of the electrons exist within the bulk InGaAs near the source as is shown in Figure 5.

The band bending is reduced at lower gate bias. The gate bias is not sufficiently strong and fewer electrons are attracted to the hetero-interface. Thus the population of the two-dimensional electron gas is much lower at the source. Figure 6 shows the layer population against the distance for different gate

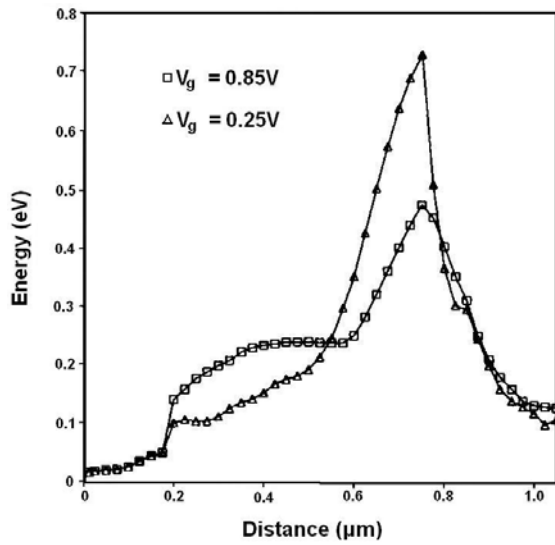


Fig. 4. Average carrier energy plotted as a function of distance along the device at gate biases of 0.25 and 0.85 V and a drain bias of 1.25 V

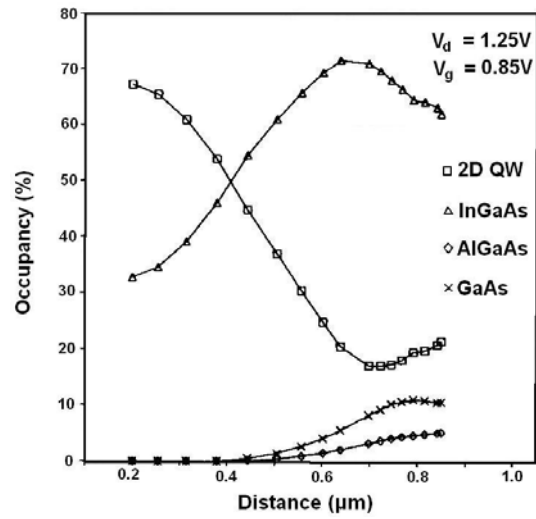


Fig. 5. Calculated layer population as a function of distance along the device at a gate bias of 0.85 V and a drain bias of 1.25 V

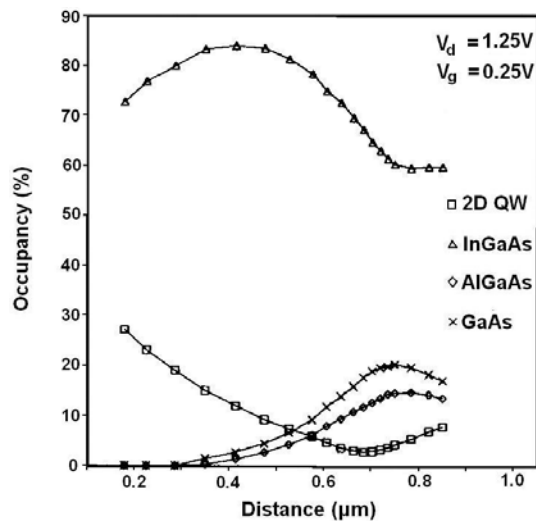


Fig. 6. Layer population as a function of distance along the device at a gate bias of 0.25 V and a drain bias of 1.25 V.

## 5. CONCLUSION

As of to date the two standard Monte Carlo algorithms, which are widely used for Monte Carlo device simulation on a semi-classical level, are the ensemble and the one-particle algorithms. The insight in the physics of the transport process has improved tremendously. A pseudomorphic HEMT structure was analysed using an ensemble Monte Carlo simulation coupled with a two-dimensional Poisson solver. The model used incorporates the physics of the device operation by including the complete transport properties of the two-dimensional electron gas, velocity overshoot and ballistic transport, real-space transfer, and the effects of the two-dimensional electric field profile, as well as the electron self-consistent field. The results are in agreement with the results from [4] and [10].

Due to the greater confinement of the electrons near the source and beneath the gate the average electron drift velocity is greater under high gate bias rather than low gate bias. The electric field increases dramatically at the drain side of the gate due to the pinch-off effect under both bias conditions. As a consequence, the electron energies increase leading to significant velocity overshoot. Electron velocities well in excess of the steady-state values are observed. The electron drift velocity drops due to the intervalley transfer in the bulk InGaAs, and real-space transfer into the surrounding lower mobility GaAs and AlGaAs layers. Depending on the gate bias, the velocity near the drain is limited by either  $k$ -space or real-space transfer. At low gate bias real-space transfer occurs, while at high gate bias intervalley transfer within the bulk InGaAs limits the carrier speeds.

## REFERENCES

1. HOCKNEY, R., Eastwood, J., *Computer Simulation Using Particles*, Bristol, Philadelphia, Adam Hilger, 1988.
2. PRICE P. J., *Two-Dimensional Electron Transport in Semiconductor Layers*, Annals of Physics, Vol. **133**, 1981, pp. 217-239.
3. BRENNAN, K. F., *Introduction to semiconductor devices*, Cambridge, Cambridge University Press, 2005
4. PARK D. H., BRENNAN K. F., *Theory of electronic transport in two-dimensional  $Ga_{0.85}In_{0.15}As/Al_{0.15}Ga_{0.85}As$  pseudomorphic structure*, Journal of Applied Physics, vol. **65**, pp. 1615-1620, 1989.
5. RAVAIOLI, U., FERRY, D. K., *MODFET ensemble Monte Carlo model including the quasi-two-dimensional electron gas*, IEEE Transactions on Electron Devices, vol. ED-**33**, pp. 677-681, 1986.
6. TOMIZAWA, K., *Numerical Simulation of Submicron Semiconductor Devices*, London, Artech House, 1993
7. JACOBONI, C., LUGLI, P., *The Monte Carlo Method for Semiconductor Device Simulation*, Wien, Springer-Verlag, 1989
8. Wordelman, C., Kwan, T., Snell C., *Comparison of Statistical Enhancement Methods for Monte Carlo Semiconductor Simulation*, IEEE Transactions on Computer-Aided Design of Integrated Circuits and Systems, vol. **17**, no. 12, pp. 1230-1235, 1998
9. AMZA, C., *Modelarea fenomenelor de transport in structuri semiconductoare utilizand metoda Monte Carlo*, PhD thesis, Bucharest, Romania, 2007
10. GELMONT B., KIM K., SHUR M., *Monte Carlo simulation of electron transport in gallium arsenide*, Journal of Applied Physics, vol. **74**, pp. 1818-1821, 1993.

Received April 22, 2008